Ian Dunn
Mem. ASME
Center for Advanced Turbomachinery and Energy Research,
Mechanical and Aerospace Engineering,
University of Central Florida,
Orlando, FL 32826
e-mail: iandunn12@knights.ucf.edu

Wilmer Flores
Mem. ASME
Center for Advanced Turbomachinery and Energy Research,
Mechanical and Aerospace Engineering,
University of Central Florida,
Orlando, FL 32826
e-mail: wflo002@knights.ucf.edu

Anthony Morales
Mem. ASME
Center for Advanced Turbomachinery and Energy Research,
Mechanical and Aerospace Engineering,
University of Central Florida,
Orlando, FL 32826
e-mail: Anthony.Morales@ucf.edu

Vidhan Malik
Center for Advanced Turbomachinery and Energy Research,
Mechanical and Aerospace Engineering,
University of Central Florida,
Orlando, FL 32826
e-mail: vidmalik@knights.ucf.edu

Kareem Ahmed
Mem. ASME
Center for Advanced Turbomachinery and Energy Research,
Mechanical and Aerospace Engineering,
University of Central Florida,
Orlando, FL 32826
e-mail: kareem.ahmed@ucf.edu

Carbon-Based Multi-Phase Rotating Detonation Engine

This article focuses on extending an H_2/air rotating detonation engine's detonability limits by introducing solid carbon particles into the combustor. Carbon black particles consisting of 1% volatility and a carbon concentration of 99% were used as a solid-phase mixing agent for enhanced reaction wave dynamics. Carbon black was found to sustain detonations over multiple operational regimes formerly unattainable without carbon particles. The experiments confirm that detonations were attainable over a wide range of operational parameters, including the total mass flux flowing through the annulus (≅120–270 kg/s m^2), the hydrogen/air equivalence ratios (0.65–1.0), and carbon additions (0–20 g). Chemiluminescence imaging was used to visualize the detonation wave within the annulus, quantify detonation wave velocities, and define a detonability map. The detonability map demonstrates the advantage of carbon addition, shows that detonation-based combustion can be sustained at leaner equivalence ratios, reduces hydrogen consumption dependency. The detonation wave velocities decreased as the H_2/air equivalence ratio was reduced, where, in general, the detonation wave velocities decreased with respect to the Chapman–Jouguet velocity, suggesting a decrease in the detonation waves efficiency with reduced H_2 concentrations. However, an extraordinary phenomenon was witnessed at very lean H_2/air equivalence ratios and low mass flux conditions, where the detonation wave velocity increased upward of 100 m/s. This variation is a direct effect of the carbon particles, which drive the detonation wave. Thus, the results demonstrate that carbon particles' addition provides an economically feasible solution to sustain high-efficiency energy production.
[DOI: 10.1115/1.4051540]

Keywords: rotating detonation engine, multiphase detonation, coal detonation, pressure gain combustion, energy conversion/systems, fuel combustion

1 Introduction

The power generation of today's global economy is dominated by three primary fuels: petroleum, natural gas, and coal. Typically, these fuels are leveraged in constant pressure thermodynamic cycles (such as the Brayton cycle), which harness deflagrations to provide sustainable energy production [1]. However, a more efficient alternative can be obtained through a constant volume combustion cycle (such as the Humphrey cycle) or a detonation cycle (the Fickett–Jacobs cycle) [1]. The Fickett–Jacobs cycle has faster chemical reaction rates over the Brayton cycle, which is particularly advantageous, and results in higher product temperatures, total pressures, and gas densities [2,3]. This is particularly advantageous as the thermodynamic cycle efficiency can increase from 27% (for a Brayton cycle) to 49% by only altering the mode of combustion [1]. In the grand scheme of power generation cycles, a Fickett–Jacobs combustion cycle can increase the total cycle efficiency by 4–6% for the simple cycle or 2–4% for the combined cycle [4]. For reference, a 1% increase in overall gas turbine cycle efficiency is equivalent to installing 17,300 wind turbines [5].

The Fickett–Jacobs cycle captures a detonation wave's mechanical work, which in turn induces pressure gain combustion (PGC) to obtain high thermodynamic cycle efficiency [1]. A detonation is a tightly confined volume, where PGC occurs when the heat released from combustion is more rapid than the gaseous expansion process [5]. If PGC devices are integrated into gas turbines, there would be an additional total pressure rise across the combustor, which would reduce the total weight of the compressor or allow for more work to be extracted from the turbines [4,5]. The most promising approach to integrate PGC into existing gas turbine systems is a rotating detonation engine (RDE). The RDE provides a favorable architecture to sustain detonations, unlike pulsed detonation engines, which require repeated ignition events to operate. Despite the associated benefits, there is a limited experimental knowledge of RDESs due to the challenge of measuring high pressure, temperature, velocities, and so on [6–8]. In addition, limited experimental data of detonation-based combustors make it challenging to develop engines suitable for energy production technologies.

Contributed by the Advanced Energy Systems Division of ASME for publication in the Journal of Energy Resources Technology. Manuscript received March 22, 2021; final manuscript received June 17, 2021; published online July 1, 2021. Assoc. Editor: Ashwani K. Gupta.

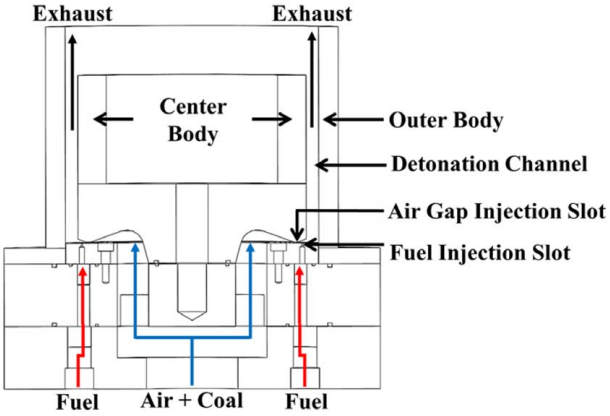

Fig. 1 RDE geometric schematic with flow pathing

One approach to controlling detonability limits given in the literature [9–13] is the use of multiphase media as a fuel source [14]. For solid–gas mixtures, there exist three subsets of particle-laden detonatable flows [9]: (1) "heterogeneous detonations" where the particle is reactive and resides in an oxidizing gaseous mixture (aluminum/oxygen) [10], (2) "hybrid detonation" where the particle is reactive, and the reaction is subsidized by a reactive gaseous mixture (hydrogen/air/coal) [11–13], and (3) "dust detonation" where an inert particle is suspended in a reactive gaseous mixture (silica/hydrogen/air) [4]. Between the three, there is particular interest in creating hybrid detonations; previous research has already shown that the use of solid media (carbon particles) creates a higher pressure rise over that of a gaseous mixture [15,16]. This insinuates an overall reduction in fuel cost and improved efficiency. The previous exploration of coal detonations by Bykovskii et al. [17] has investigated hydrogen–coal, multiphase, planar spin continuous detonations using cannel coal at particle sizes from 1 to 7 μm. Operational regimes were tested and plotted to create a map where continuous spin detonations existed. Concentration amounts of coal to hydrogen varied from 53% to 97.7% by mass, where it was found that the "most chemically active mixtures" and highest number of detonation waves ($n = 6$) occurred at the richest hydrogen equivalence ratios ($\varphi H_2 \cong 0.4$). The research also attempted to deduce the detonation wave velocities via imaging that had long exposures and streaked detonation waves. The research proved that a solid-gaseous detonation cycle could exist within a confined engine, thus proving the feasibility of a carbon-based fuel within an RDE.

Thus, this research aims to extend the knowledge of detonability limits in an RDE utilizing solid-phase media. Specifically, detonability limits are experimentally quantified utilizing carbon within a modern RDE. A comprehensive experimental assessment of hybrid detonation limits was evaluated using chemiluminescence to quantify detonation wave speeds across various mass fluxes, equivalence ratios, and carbon concentrations. These values were directly compared to the detonability limits of a pure H_2/air interaction and were found that with the addition of carbon, detonability limits were increased.

2 Experiment and Methodology

2.1 Rotating Detonation Engine. The RDE utilized in this study was modeled after the Air Force Research Laboratories [6], which is shown in Fig. 1. Air, coal, and hydrogen enter the RDE from various cavities located at the bottom. Air and coal are radially injected from a circumferential slot with an area of 212.9028 mm^2. Hydrogen is fed axially in the detonation channel through 80 discrete circular injection orifices with 0.89 mm diameters. The fuel injectors impinge on the air slot gap to induce rapid mixing. The mixture flows through a channel gap of 7.62 mm. The RDE is a recessed inner body to improve aerodynamic performance [18].

A predetonator was utilized as the RDE's ignition source, filled with H_2/Air reactants, and ignited. The propagating flame is accelerated by a pseudo-Schelkin spiral, which induces a deflagration to detonation transition. The incipient detonation wave ignites the RDE.

2.2 Flow Network. A schematic of the experimental setup is provided in Fig. 2. Compressed air is fed from a bottle farm and flows through a dome-loaded TESCOM 26–1200 pressure regulator. The dome-loaded pressure regulator is controlled by an auxiliary PID-tuned TESCOM 44–1300 pressure regulator to control the flow autonomously. A pressure transducer and thermocouple measure the downstream pressure and temperature before the flow enters a restriction orifice union. The upstream and downstream pressure readings are used to meter the mass flow into the system, where the dome regulator setpoint is adjusted to meet parametric flow conditions. The fuel line design mimics the air line; however, there is one notable difference. After the restriction orifice union, the fuel line splits from a single pipe into a fuel manifold where hydrogen fuel is supplied to the RDE with six high-pressure rubber hoses.

The solid carbon media is injected through an inline seeder, which allows a portion of air to pass through and lift particles

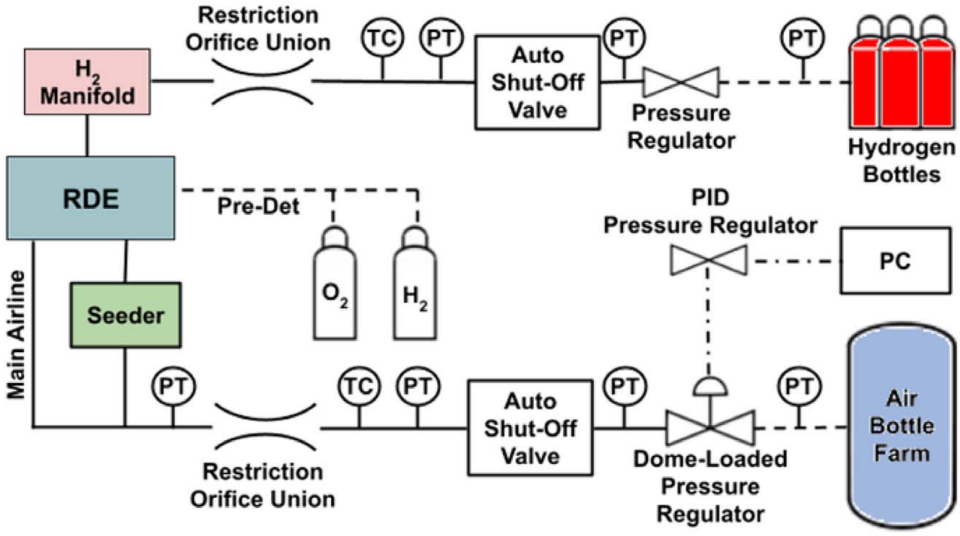

Fig. 2 Flow facility features and mapping

from the bed's surface. Carbon was premixed with air to decrease the level of circumferential stratification across the annulus of the RDE. The carbon was intentionally mixed within the airline to increase experimental detonation wave velocities compared to Chapman–Jouguet (CJ) wave velocities [19–21]. Additional details about the inline seeder are described in Sec. 2.3.

2.3 Inline Seeder and Coal. Figure 3 shows a schematic of the seeder's internal structuring and an isometric view of the downstream conditioning. Airflow enters from the bottom and is choked by a set of sonic orifices. Low-volatility coal particles (~1% volatility, ~99% carbon, 29 ± 10 nm diameter), known as carbon black, were mixed with air to create a premixed multiphase mixture. Particles were initially measured utilizing a GEMINI-20 scale with a resolution of 1 mg. Mie-scattered images were used to confirm a uniform seed-to-air density through an entire run.

2.4 High-Speed Imaging. Chemiluminescence imaging of the RDE's channel captures the detonation behavior from backend imaging. An angled mirror was positioned downstream from the backend of the RDE at a 45-deg angle. A high-speed CMOS camera (Photron Fastcam SA 1.1) was pointed at the mirror to capture images at 67,500 frames per second (FPS). The image's resolutions were 256×256 pixels and were exposed at a time of 1/FPS. A variable focal length (70–300 mm) Nikon lens with an f-stop *f*/1.4 magnified a spatial resolution of 0.73 mm/pixel. Figure 4 shows a raw image of detonation waves traveling the annulus. The detonation wave is a discrete pocket of luminescence, where the width of the wave is 12 pixels across the annulus, creating a large enough signature to capture wave dynamics accurately.

2.5 Quantification of Detonation Wave Velocity. A processing technique created by Bennewitz et al. [22] was utilized to capture detonation wave dynamics; the algorithm uses chemiluminescence to identify the number of waves and quantify detonation

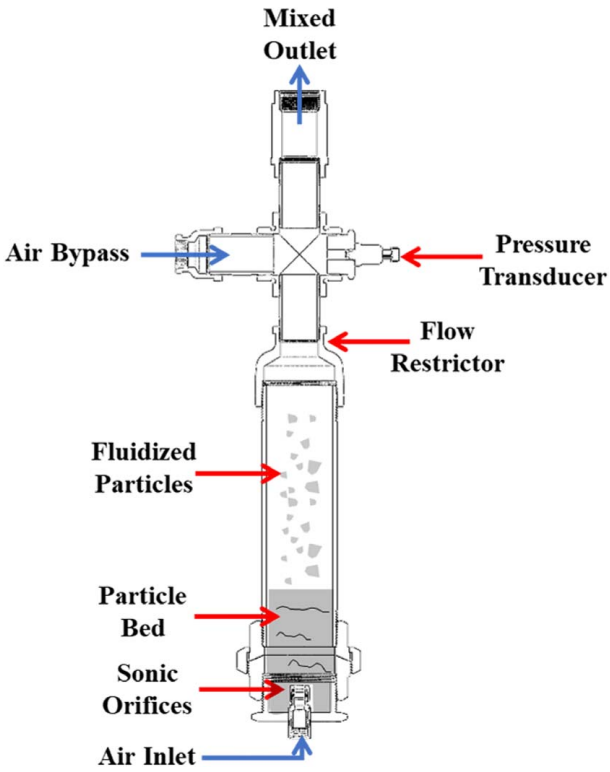

Fig. 3 Inline seeder to flow coal into the RDE

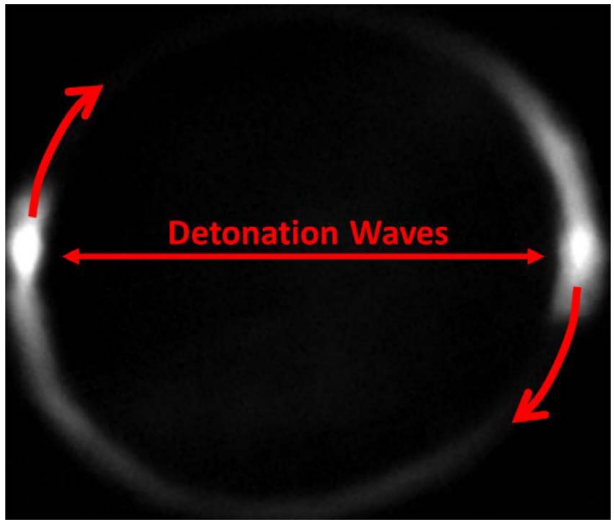

Fig. 4 Raw image of the detonation waves rotating the annulus

wave velocities. The algorithm leverages an image-processing technique consisting of (1) background subtraction, (2) intensity normalization, and (3) a spatial/temporal discrete Fourier transform (DFT). Knowing both the number of waves and the frequency spectra from the DFT, the detonation wave velocity can be calculated as follows:

$$U_{DW} = \frac{\pi * D_{\text{Mean}} * f_{\text{Max}}}{n_{\text{Wave(s)}}} \tag{1}$$

The frequency resolution of the DFT is based on the samples provided and the frequency of sampling. To accurately depict a dominating mode of operation within the annulus of the RDE, a sample of 5000 images was input. By using the specified sample size and the frequency of the camera (67,500 FPS), this resulted in a DFT resolution of 13.5 Hz, which correlated with a difference in detonation wave velocity of ±3.1 m/s (<1% uncertainty to resolved detonation velocities).

3 Multiphase Detonation Analysis

Combustion in an RDE is typically classified with three dominant modes: (a) deflagration, (b) longitudinally pulsed detonation, and (c) stable detonations. The operational modes are depicted in Fig. 5, where Fig. 5(*a*) shows the nonreacting exhaust plume filled with coal as it exits the engine. Figure 5(*b*) shows a deflagration, a slow reaction without PGC, and is the least-efficient heat release method within an RDE. Longitudinally pulsed detonations (LPDs), not depicted in Fig. 5, are instability caused by shock reflections developed from a malformed detonation wave structure. This instability is caused by shocks traveling upstream into the injection plate of the RDE, which reignite and detonate, causing the LPD cycle to repeat [23]. LPDs naturally exist between stable and unstable regimes and are considered a transitional mode of operation. Finally, Fig. 5(*c*) shows detonations that are a discrete pocket of highly reactive gas mixtures traveling at supersonic speeds, which produce PGC and are the most efficient mode of heat release within an RDE. The RDE is considered operational when sustained and stabilized detonation(s) form and continuously travel the annulus.

Although the images in Fig. 5 show a clear detonation mode of the RDE using coal injection, the detonation operability is quantitatively assessed using backend imaging. An example of the detonation wave velocity analysis is displayed in Fig. 6. The slope of the dashed line within the waterfall plot represents the detonation wave velocities as they travel the annulus. Also, a vertical slice at any instant of time will show the instantaneous of the detonation wave(s).

Fig. 5 Exact concentrations of carbon versus hydrogen/air equivalence ratio where an average carbon concentration capturing multiple mass flux conditions is established: (*a*) coal injection, nonreacting, (*b*) deflagration, and (*c*) detonation

3.1 Coal Concentrations. Experimental conditions tested within this investigation are described as shown in Fig. 7. Each of the three different carbon mass test points was run over five different H_2/air equivalence ratios and three mass fluxes (45 tests in total). The experiments confirm that detonations were attainable over a wide range of operational parameters, including the total mass flux flowing through the annulus (≅120–270 kg/m^{2}s), the hydrogen/air equivalence ratios (0.65–1.0), and carbon concentrations (0–20 g per second).

3.2 Low Mass Flux (≅120 kg/(s*m^2)). The detonability limits for the low max flux case, 120 kg/m^{2}s, are provided in Fig. 8. It is first noted, without any carbon addition, that the lowest H_2/air equivalence ratio to detonate exists at an equivalence of 0.8. As 10 g of carbon are added to the reactant mixture, a phenomenon exists, where the detonability limit is extended by 23%, down to an H_2/air equivalence of 0.65. This is economically advantageous as the elimination of hydrogen dependence reduces overall cost within a power generation cycle. However, with the addition of 20 g into the detonation wave, overall operability limits decreased, as shown by an increase in H_2/air equivalence ratio of 0.8 (toward the baseline case). This is likely due to the oversaturation of carbon particles, as previously observed by Zhang et al. [24]. The ideal operational point exists at an H_2/air equivalence ratio of 0.65 and 10 g of carbon addition based on the data.

Detonation wave velocities are provided in Fig. 8(*b*) and also compared to CJ detonation wave velocities. All CJ wave velocities were computed on NASA's Chemical Equilibrium and Applications thermodynamic calculator [25], where the computed velocities are assumed to be a gas-to-gas interaction, not a solid-to-gas interaction. There is a general decaying trend of detonation velocities within the low mass flux regime as H_2/air equivalence ratios decrease or carbon addition increases. Initially, the detonation waves are shown to be sensitive to the H_2/air equivalence ratio; however, for H_2/air < 0.8, the detonations must be driven by the carbon addition. In other words, the physical mechanism that sustains the detonation is caused by the shift of the supporting reactive material from hydrogen to carbon. This phenomenon has been previously documented using a pulse detonation engine, where a pure thermodynamic approach discerned that there is an optimal carbon addition concentration [26,27] as depicted by the 10-g carbon addition and 0.65 H_2/air equivalence ratio.

3.3 Medium Mass Flux (≅170 kg/(s*m^2)). Figure 9 shows similar operability limits and detonation wave velocities as shown in Fig. 8. Overall concentrations of carbon have decreased due to hydrogen's higher mass flow required to sustain the desired equivalence ratios. Unlike the low mass flux case, the pure H_2/air mixtures detonated at lower equivalence ratios of 0.7 and 0.65. This is expected to be the result of a total increase of mass flux (and the total number of moles of hydrogen), increasing the total enthalpy of the mixture. In this case, the additional energy supplied at low equivalence ratios can form and sustain a detonation wave. In contrast, quenching still occurs despite the increase in enthalpy supplied to the mixture. However, if the volatility of the coal changed, from the original ∼1% (carbon black) to that of ∼20% (subbituminous coal) at the same size, these limits would certainly be pushed out into leaner hydrogen/air equivalence ratios [26,27].

Similar to the low mass flux case, as the H_2/air equivalence ratio decreases, so do the associated detonation wave velocity shown in Fig. 9. Contrasting the low mass flux case, detonation velocities

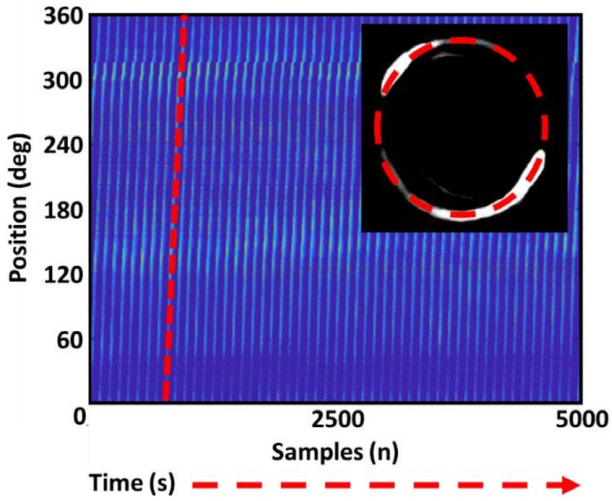

Fig. 6 Corrected image of detonation waves rotating annulus with a waterfall plot backdrop showing velocities based on slope (dashed line) and number of waves existing at once

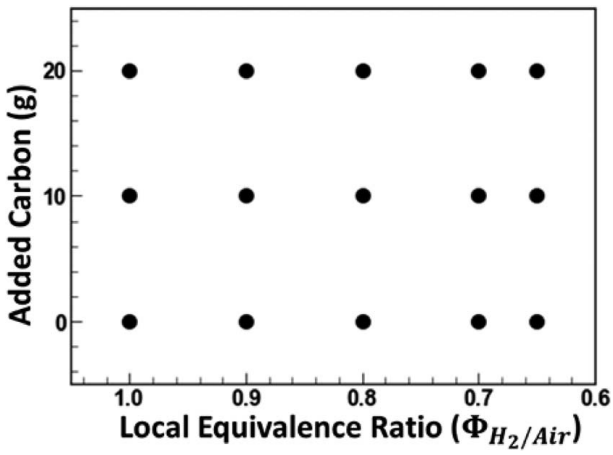

Fig. 7 Experimental test conditions, showing the amount of carbon added to the reactants and H_2/air equivalence ratio. The same conditions are run for each mas flux: 120, 170, and 270 kg/m^2 s.

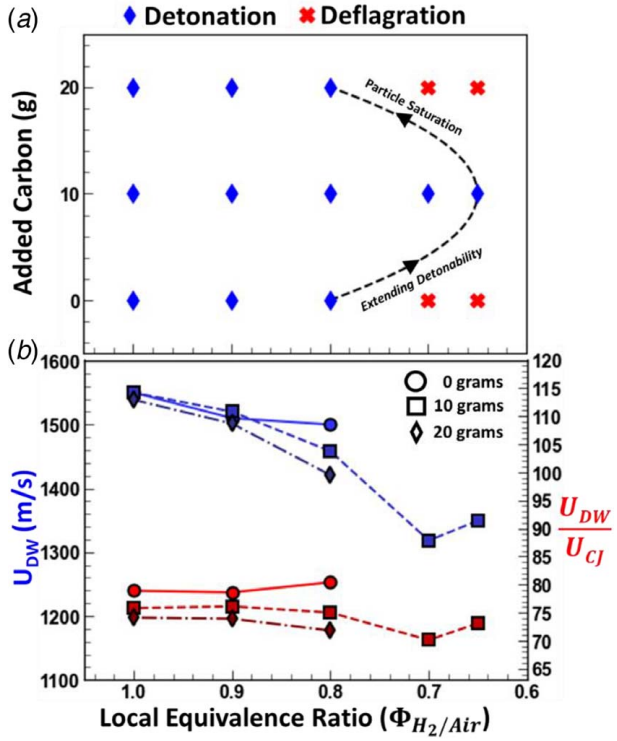

Fig. 8 Concentrations of carbon versus H_2/air equivalence ratios (*a*). Detonation velocities and ratios of CJ velocities compared to detonation velocities are shown against equivalence ratios (*b*). Both graphs' present operational parameter at ≅120 kg/(s*m^2) mass flux.

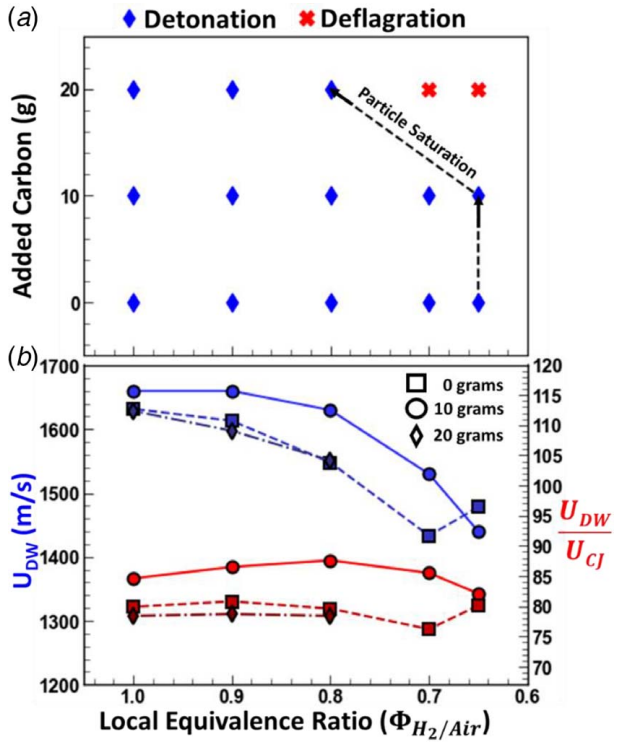

Fig. 9 Concentrations of carbon versus H_2/air equivalence ratios (*a*). Detonation velocities and ratios of CJ velocities compared to detonation velocities are shown against equivalence ratios (*b*). Both graphs' present operational parameter at ≅170 kg/(s*m^2) mass flux.

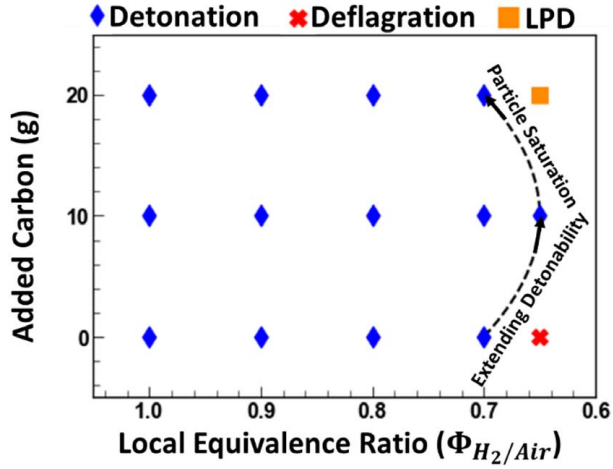

Fig. 10 Concentrations of carbon versus H_2/air equivalence ratios (top). The graph presents operational parameters at ≅270 kg/(s*m^2) mass flux.

have increased overall by at least ~100 m/s caused by the total enthalpy supplied to the mixture. At 20 g of carbon addition, the detonation wave velocities do not experience an almost ~2–3% decrease compared to CJ velocity, as shown in Fig. 8, but remain constant until deflagration occurs. The carbon-driven detonation wave occurs at the same condition as the low mass flux case and is highlighted by the detonation wave increase over the baseline case.

3.4 High Mass Flux (≅270 kg/(s*m^2)). Figure 10 displays the final mass flux studied, where H_2 is increased while the amount of carbon addition is held static. Gas velocity in the annulus of the RDE increases with the increase of mass flux, where malformed detonations cannot anchor on the fuel plenum and are pushed out as a deflagration [6]. Thus, in comparison to the medium mass flux, baseline detonability limits decreased while the addition of 10 g of carbon remained the same, further insinuating that carbon is supporting the detonation wave. At high mass concentrations (20 g and 0.7 H_2/air equivalence ratio), detonability increases over that of the low and medium mass fluxes and is realized by

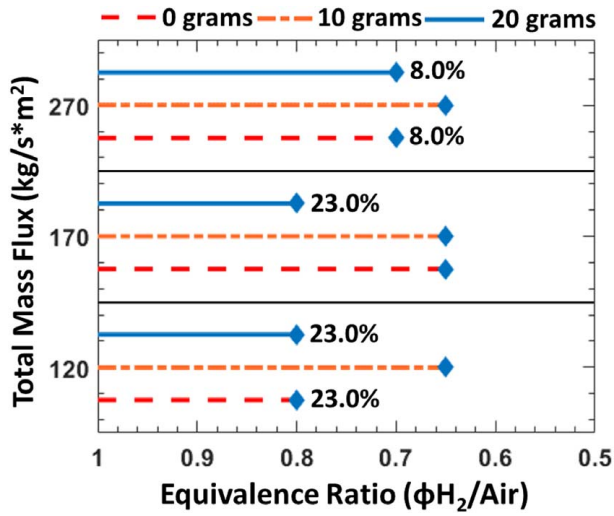

Fig. 11 Mass flux in comparison to hydrogen/air equivalence ratio. Percentage difference inset within the graph depicting reduction of operability compared to the leanest operating condition within the same mass flux.

the onset of LPDs rather than deflagrations. Detonation velocities were not depicted due to the extreme density of particles laden in the flow. However, small sectors of the annulus were visible for a short time, depicted by the backend imaging, which gave detonability confirmation.

3.5 Comparative Operational Map. Figure 11 shows the culmination of the leanest H_2/air equivalence ratios that detonated per mass flux and carbon addition. At every mass flux, with the addition of 10 g of carbon, overall operability increased compared to baseline, which reduces the required amount of H_2 addition upward of 23% for stable operation. Also, with the continuous addition of carbon concentration, operability is negatively affected, and detonations cannot form Ref. [24]. Thus, doping a detonation wave with carbon is a proficient solution to reduce operation costs and increase operability.

4 Conclusions

The first evidence of a solid–gas multiphase rotating denotation engine was presented in this study. This investigation has validated the ability to use carbon particles to increase the lean-limit operability regime. A coal-driven RDE was explored for various carbon concentrations, lean and stoichiometric equivalence ratios, and various mass fluxes.

With the addition of carbon, lean detonability limits have increased. Lean detonability increase is significant at lower mass fluxes, where carbon addition by weight is more impactful than at higher mass fluxes, noted as a 23% increase in operability over the baseline H_2/air detonability limit. However, with a further increase past a critical carbon addition concentration (from 10 to 20 g), operability decreases due to immense carbon loading to the detonation front previously denoted by numerous hybrid detonation investigations.

Detonation wave velocities were discerned through backend imaging of the annulus. It was found that a general decrease in detonation wave velocity occurred with the reduction of H_2/air; however, at low H_2/air equivalence ratios (0.65) and low-to-medium mass fluxes, with the addition of carbon (10 g), detonation wave velocity increased. This is caused by a shift in the physical mechanism driving the detonation wave, where the supporting reactive material becomes carbon and not hydrogen.

Funding Data

- Department of Energy National Energy Technology Laboratory for Advanced Combustion Systems (DE-FE0031545).

Conflict of Interest

There are no conflicts of interest.

Data Availability Statement

The datasets generated and supporting the findings of this article are obtainable from the corresponding author upon reasonable request. The authors attest that all data for this study are included in the paper. No data, models, or code were generated or used for this paper.

Nomenclature

C = carbon
f_{Max} = maximum frequency observed within discrete Fourier transform
$n_{Wave(s)}$ = number of waves traveling the annulus
H_2 = hydrogen
D_{Mean} = mean diameter of annulus
U_{CJ} = Chapman–Jouguet wave velocity
U_{DW} = detonation wave velocity
CJ = Chapman–Jouguet
$\Phi_{H_2/Air}$ = equivalence ratio of hydrogen to air

References

[1] Kailasanath, K., 2000, "Review of Propulsion Applications of Detonation Waves," AIAA J., **38**(9), pp. 1698–1708.
[2] Turns, S., 2000, *An Introduction to Combustion: Concepts and Applications*, McGraw Hill, New York.
[3] Kuo, K., 2005, *Principles of Combustion*, Wiley Interscience, Hoboken, NJ.
[4] Desmira, N., Nagasaka, T., Narukawa, K., Ishikawa, A., Kitagawa, K., and Gupta, A. K., 2013, "Spectroscopic Observation of Chemical Species From High-Temperature Air Pulverized Coal Combustion," ASME J. Energy Resour. Technol., **135**(3), p. 034503.
[5] Paxson, D., 2018, "Pressure-Gain Combustion for Gas Turbines," ASME 2018 Turbo Expo, ASME, Lillestrom, Norway, June 11–15.
[6] Rankin, B., Richardson, D., Caswell, A., Naples, A., Hoke, J., and Schauer, F., 2017, "Chemiluminescence Imaging of an Optically Accessible Non-Premixed Rotating Detonation Engine," Combust. Flame, **176**, pp. 12–22.
[7] Pal, P., Kumar, G., Drennan, S. A., Rankin, B. A., and Som, S., 2021, "Multidimensional Numerical Modeling of Combustion Dynamics in a Non-Premixed Rotating Detonation Engine With Adaptive Mesh Refinement," ASME J. Energy Resour. Technol., **143**(11), p. 112308.
[8] Fugger, C. A., Lopez, J. G., Rein, K. D., Roy, S., and Caswell, A. W., 2021, "The Dynamics of a Non-Premixed Rotating Detonation Engine From Time-Resolved Temperature Measurements," Proc. Combust. Inst., **38**(3), pp. 3787–3795.
[9] Zhang, F., 2009, "Detonation of Gas-Particle Flow," Shock Wave Sci. Technol. Ref. Libr., **4**, pp. 87–168.
[10] Strauss, W., 1968, "Investigation of the Detonation of Aluminum Powder–Oxygen Mixtures," AIAA J., **6**(9), pp. 1753–1756.
[11] Veyssiere, B., and Manson, N., 1982, "Sur l'existence d'un second front de détonation des mélanges biphasiques hydrogène-oxygène-azote-particules d'aluminium," C. R. Acad. Sci., **295**(2), pp. 335–338.
[12] Veyssiere, B., 1986, "Structure of the Detonations in Gaseous Mixtures Containing Aluminum Particles in Suspension," Prog. Astronaut. Aeronaut., **106**, pp. 522–544.
[13] Zhang, F., Thibault, P., and Murray, S. B., 1998, "Transition From Deflagration to Detonation in an End Multiphase Slug," Combust. Flame, **114**(1–2), pp. 13–25.
[14] Ma, H., Zhou, L., Lv, S., Chew, J. W., and Wang, Z., 2019, "Review on Reaction Mechanisms of Sulfur Species During Coal Combustion," ASME J. Energy Resour. Technol., **141**(10), p. 100801.
[15] Denkevits, A., 2007, "Explosibility of Hydrogen–Graphite Dust Hybrid Mixtures," J. Loss Prev. Process Ind., **20**(4–6), pp. 698–707.
[16] Li, Q., Lin, B., Dai, H., and Zhao, S., 2012, "Explosion Characteristics of H2/CH4/Air and CH4/Coal Dust/Air Mixtures," Powder Technol., **229**, pp. 222–228.
[17] Bykovskii, F. A., Zhdan, S. A., Vedernikov, E. F., and Zholobov, Y. A., 2013, "Continuous Spin Detonation of a Coal–Air Mixture in a Flow-Type Plane–Radial Combustor," Combust., Explos. Shock Waves, **49**(6), pp. 705–711.
[18] Fotia, M., Schauer, F., Kaemming, T., and Hoke, J., 2016, "Experimental Study of the Performance of a Rotating Detonation Engine With Nozzle," J. Propul. Power, **32**(3), pp. 674–681.
[19] Thomas, G. O., Sutton, P., and Edwards, D. H., 1991, "The Behavior of Detonation Waves at Concentration Gradients," Combust. Flame, **84**(3–4), pp. 312–322.
[20] Ishii, K., and Kojima, M., 2017, "Behavior of Detonation Propagation in Mixtures With Concentration Gradients," Shock Waves, **17**(1–2), pp. 95–102.
[21] Boeck, L. R., Berger, F. M., Hasslberger, J., and Sattelmayer, T., 2016, "Detonation Propagation in Hydrogen–Air Mixtures with Transverse Concentration Gradients," Shock Waves, **26**(2), pp. 181–192.
[22] Bennewitz, J. W., Bigler, B. R., Hargus, W. A., Danczyk, S. A., and Smith, R. D., 2018, "Characterization of Detonation Wave Propagation in a Rotating Detonation Rocket Engine Using Direct High-Speed Imaging," AIAA Propulsion & Energy, Cincinnati, OH, July 9–11.
[23] Anand, V., George, A., Driscoll, R., and Gutmark, E., 2016, "Longitudinal Pulsed Detonation Instability in a Rotating Detonation Combustor," Exp. Therm. Fluid. Sci., **77**, pp. 212–225.
[24] Zhang, F., Murray, S., and Gerrard, K., 2003, "Hybrid Detonations in Aluminum Dust–Gas Mixtures," Proceedings of the 19th International Colloquium on the Dynamics of Explosions and Reactive Systems, Hakone, Japan, July 27–Aug. 1, pp. 167.161–167.164.
[25] Gordon, S., and McBride, B., 1996, *Computer Program for Calculation of Complex Chemical Equilibrium Compositions and Applications*, NASA Reference Publication, Cleveland, OH, p. 1311.
[26] Veyssière, B., Kasainov, B., Mellas, B., and Daniau, E., 2006, "Performance of Propellant Decomposition Products as Fuel in an Airbreathing PDE," Shock Waves, **16**(2), pp. 149–156.
[27] Khasainov, B., and Veyssiere, B., 1988, "Steady, Plane, Double-Front Detonations in Gaseous Detonable Mixtures Containing a Suspension of Aluminum Particles," Dyn. Explos, **114**, pp. 284–299.